Semi-Supervised vs. Supervised Learning for Discriminating Atrial Flutter Mechanisms Using the 12-lead ECG

Giorgio Luongo[1], Steffen Schuler[1], Massimo W Rivolta[2], Olaf Dössel[1], Roberto Sassi[2], Axel Loewe[1]

[1]Institute of Biomedical Engineering, Karlsruhe Institute of Technology (KIT), Karlsruhe, Germany
[2]Dipartimento di Informatica, Università degli Studi di Milano, Milan, Italy

Abstract

Atrial flutter (AFl) is a common heart rhythm disorder driven by different self-sustaining electrophysiological atrial mechanisms. In this work, we tried to automatically distinguish the macro-mechanism sustaining the arrhythmia in an individual patient using the non-invasive 12-lead electrocardiogram (ECG). We implemented a concurrent clustering and classification algorithm (CCC) to discriminate the clinical classes and look for potential similarities between patient features in each class, thus suggesting that these patients would require a similar treatment. The CCC performance was then compared to a standard supervised technique (K-nearest neighbor, KNN). 3-class classification (macro-reentry right atrium, macro-reentry left atrium, and others) achieved 48.3% and 72.0% CCC and KNN accuracy, respectively. 4-class classification (tricuspidal reentry, mitral reentry, fig-8 macro-reentry, and others) achieved 41.6% and 71.2% CCC and KNN accuracy, respectively. Our results show that a clustering approach does not improve the performance of AFl classification because the semi-supervised method leads to clusters that are strongly overlapping between the different ground truth classes. In contrast, the supervised learning approach shows potential for the classification, although constrained by the complexity and the multiple variables that influence the underlying mechanisms.

1. Introduction

Atrial flutter (AFl) is a common arrhythmia that can be categorized according to different self-sustained electrophysiological mechanisms driving it. This atrial tachycardia is characterized by electrical signals that repeatedly propagate along various physiological pathways different from sinus rhythm [1]. Although AFl is not directly lethal, it can lead to significant complications and symptoms - e.g., palpitations, dyspnea, stroke and heart attack. The most used treatment to restore sinus rhythm from AFl conditions is ablation therapy. Each AFl mechanism requires a different ablation procedure [2].

To identify the AFl mechanism in an individual patient, invasive mapping of the atria's electrical activity is carried out using intracardiac catheters. In addition, the 12-lead ECG is also collected during the intervention. The use of the surface ECG to identify the mechanism of AFl would facilitate patient selection, the planning of the intervention and reduce the procedure time for invasive mapping and ablation therapy. An automatic identification of different AFl mechanisms using only the 12-lead ECGs was attempted in one of our previous works [3], reaching promising performance.

In this study, we investigated the possibility of identifying clusters of patients with ECGs displaying similar feature behaviors within the same ground truth class (clinical classes) and thereby aiding in the automatic classification of the clinical classes themselves. This clustering can be automatically performed by means of algorithms belonging to the unsupervised learning domain. Using this unsupervised method within already clinically defined classes led us to refer to a semi-supervised approach. Here, we tested an algorithm that could concurrently cluster and classify (CCC) the ECG of a patient during AFl. The algorithm aims to estimate the type of AFl mechanism, as well as the cluster (or, in other words, the patient group). We compared this algorithm with a supervised K-nearest neighbor (KNN) classifier.

2. Methods

2.1. Simulated AFl scenarios

Based on the AFl simulations implemented in our previous work [4], a database of computational AFl scenarios was set up. The complete list of scenarios is provided in Table 1.

Cardiac excitation was simulated using the fast marching approach to solve the Eikonal equation [5,6]. The atrial electrophysiological activity was simulated on tetrahedral volume meshes of 8 bi-atrial anatomies, generated from segmented magnetic resonance imaging data of healthy

Table 1. Database of clinically informed manually parameterized AFl mechanisms

Mechanism	Atrium	Position	Direction	3cc	4cc
Macro-reentry	RA	Tricuspid Valve	ccw	I	I
Macro-reentry	RA	Tricuspid Valve	cw	I	I
Macro-reentry	LA	Mitral Valve	ccw	II	II
Macro-reentry	LA	Mitral Valve	cw	II	II
Scar-related Reentry	LA	LPV	post	II	IV
Scar-related Reentry	LA	LPV	ant	II	IV
Scar-related Reentry	LA	RPV	post	II	IV
Scar-related Reentry	LA	RPV	ant	II	IV
Figure-8 Macro-reentry	LA	Both PVs	ant	II	III
Figure-8 Macro-reentry	LA	Both PVs	post	II	III
Figure-8 Macro-reentry	LA	RPVs	ant	II	III
Focal Source	LA	RSPV anterior		III	IV
Focal Source	LA	RSPV posterior		III	IV
Focal Source	LA	LSPV anterior		III	IV
Focal Source	LA	LSPV posterior		III	IV
Micro-reentry	LA	ant MV annulus		III	IV
Micro-reentry	LA	ant LAA		III	IV
Micro-reentry	LA	ant RSPV		III	IV
Figure-8 Micro-reentry	LA	ant		III	IV
Micro-reentry	LA	post wall		III	IV

Right atrium (RA), left atrium (LA), left pulmonary veins (LPV), right pulmonary veins (RPV), pulmonary veins (PVs), right superior pulmonary vein (RSPV), left superior pulmonary vein (LSPV), mitral valve (MV), left atrial appendage (LAA), clockwise (cw), counterclockwise (ccw), anterior (ant), posterior (post), 3-clinical-class (3cc) classification, 4-clinical-class (4cc) classification.

male and female subjects [7].

Transmembrane voltages (TMV) were obtained using the Courtemanche *et al.* mathematical model of the human atrial action potential, including chronic atrial fibrillation-induced remodeling [8]. From the TMV, the body surface potential map (BSPM) was calculated on 8 different torso surface models using the boundary element method. To augment the dataset, atria were placed within the torso using two different orientations. From the BSPM, the 12-lead ECG was extracted. A detailed description of the simulation procedure can be found in [4].

Each 12-lead ECG signal covered a single AFl cycle and was sampled at 1 kHz. ECG signals were formed only by F-waves without the QRS complex and T-wave (representing ventricular activity) since the ventricles were not included in the simulations. Figure 1) shows examples of single cycle ECG signals.

A total of 2,512 12-lead ECGs were calculated from the simulated AFl scenarios on 8 atrial models with 2 orientations and 8 torso models.

2.2. Feature extraction and selection

151 features were extracted from the 12-lead ECGs using several biosignal processing methods from different domains, e.g., time, frequency, wavelet, entropy, and nonlinear recurrence analysis. All features were min-max normalized.

A greedy forward selection algorithm was implemented to select a feature set using the KNN algorithm (see sec. 2.3). This algorithm started with an empty feature set and added the feature leading to the highest increase in accuracy to the set at each iteration. The algorithm was stopped when performance based on the validation set could not be further increased. To avoid feature redundancy, the candidate feature was only added if the correlation coefficient with any of the already included features was < 0.6. Feature selection was performed to have a relevant feature set to be tested with CCC.

2.3. Classification

Two classification problems were investigated. The first one involved 3 clinical classes (3cc) while the second one considered 4 clinical classes (4cc). The simulated AFl mechanisms were grouped based on the classification problem. 3cc considered macro-reentry RA (I), macro-reentry LA (II), and others (III). 4cc was defined with tricuspidal-reentry (I), mitral-reentry (II), fig-8 macro-reentry (III), and others (IV). Table 1 show to which clinical class each AFl scenario was assigned (columns 3cc and 4cc).

CCC and KNN classifiers were implemented for both classification problems. For both classifiers, 6 random atrial anatomical models were used for the training set, 1 atrial model for the validation set, and the remaining atrial model for the test set. This prevented overfitting to the atrial models used in this study [3]. CCC and KNN used the same feature set previously selected using only the training and validation sets. The number of neighbors used by the KNN was iteratively optimized on the validation set performance (optimal neighbors' number was set to 6 and 4 for 3cc and 4cc, respectively).

The CCC was implemented following the directions of Rivolta *et al.* [9]. In each clinical class, 3, 5, and 7 clusters were calculated using k-means to identify similarities between patients within the same clinical class. The k-means algorithm was repeated 100 times and the clusters' centroids displaying the largest distance between each other were retained. The clusters identified in each clinical class were then combined in feature space to obtain the classifier. Each test sample was assigned to the clusters with smallest distance between the centroid and the test sample itself. The test sample was thus automatically identified as the clinical class to which the cluster belongs.

Performance was assessed using the accuracy performance metric.

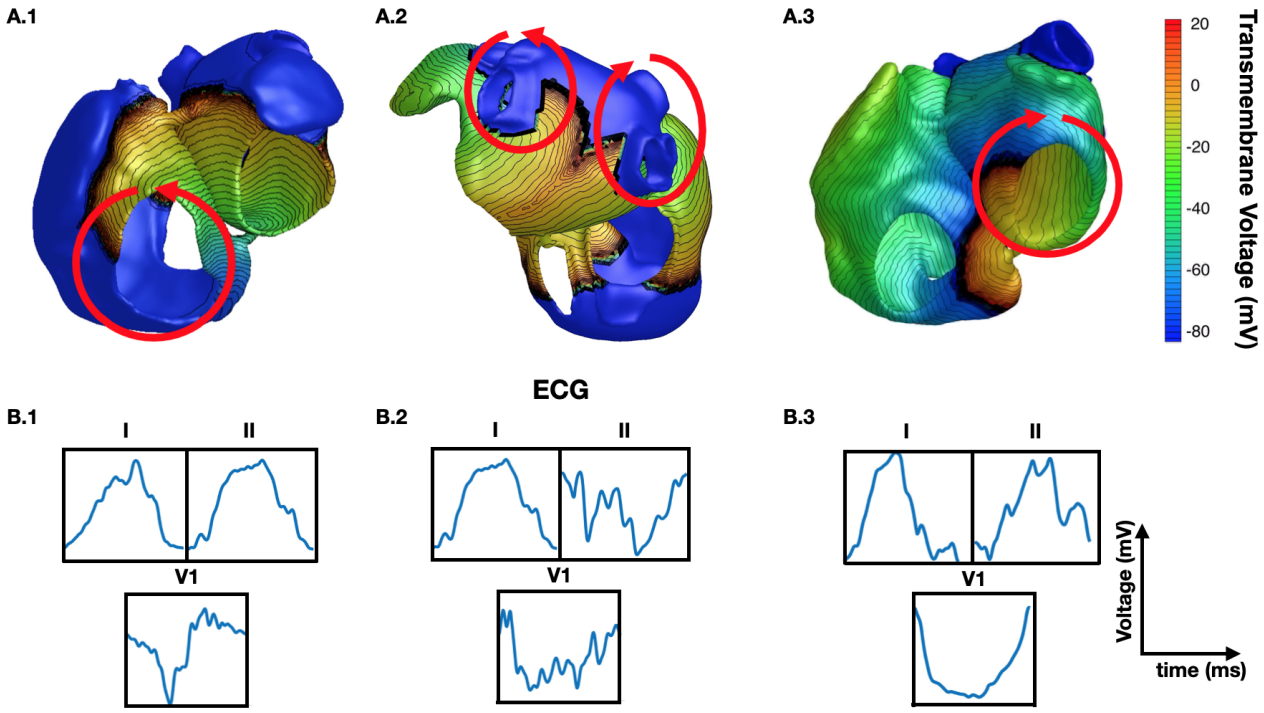

Figure 1. A.1. Simulated macro-reentry AFl around the tricuspid valve with ccw direction of rotation (red arrow). A.2. Simulated figure-8 macro-reentry AFl around the left and right PVs with anterior direction of rotation (red arrows). A.3. Simulated macro-reentry AFl around the mitral valve with cw direction of rotation (red arrow). B. Example of the F-wave single cycle ECG for leads I, II, and V1 of the 12-lead ECG extracted from the BSPM.

3. Results

Accuracy did not improve significantly with more than 2 features for both classification problems. Therefore, we report only the results for this case here to facilitate the 2 dimensional visualization of the behaviour of CCC (2).

The selected 3cc feature set was: F-wave duration (cycle length) and trapping time (TT) of the third principal component obtained by PCA of the 12-lead ECG calculated with Individual Component Recurrence Quantification analysis (icRQA) [4]. On the other hand, the 4cc feature set was: F-wave duration and laminarity (LAM) of the second principal component calculated with icRQA.

For the 3cc problem, CCC achieved 50.5%, 45.4%, and 48.3% accuracy on the test set calculated with 9, 15, and 21 total clusters (3, 5, and 7 clusters for each clinical class, respectively). In comparison, the KNN classifier achieved a test set accuracy of 72.0%. Regarding the 4cc problem, the CCC classifier achieved 34.7%, 38.1%, and 41.6% accuracy on the test set with 12, 20, 28 total clusters (3, 5, and 7 clusters per clinical class, respectively). One the other hand, the KNN classifier achieved 71.2% test accuracy.

Figure 2 shows two examples of the partitioning of the feature space into clusters and their clinical classes using k-means, and the position of the test set samples.

4. Discussion and Conclusions

Simulations provide ideal and controlled scenarios where the ground truth mechanism driving AFl is known in all cases, allowing for the analysis of each mechanism without the influence of secondary - or unknown - mechanisms. The classification by CCC led to a drastic reduction in performance compared to the KNN classifier for both classification problems. The clustering within each clinical class was not able to distinguish between all others correctly.

This can be seen from the examples in Fig 2 since there is not a clear match between test samples scattered in the feature space and the calculated clusters. Given the autonomous and uncontrolled nature of clustering in partitioning the data, the resulting clusters revealed differences among the dataset that were not useful for the classification, even if we used a semi-supervised method. Moreover, the idea of using the clusters identified to perform classification was probably too coarse (feature values were overlapping too much). Increasing the number of clusters might have ameliorated the situation but at the cost of interpretability of the results, and, at the end of the day, would have thwarted the clustering idea itself by converging into a KNN. In contrast, the KNN classifier results showed

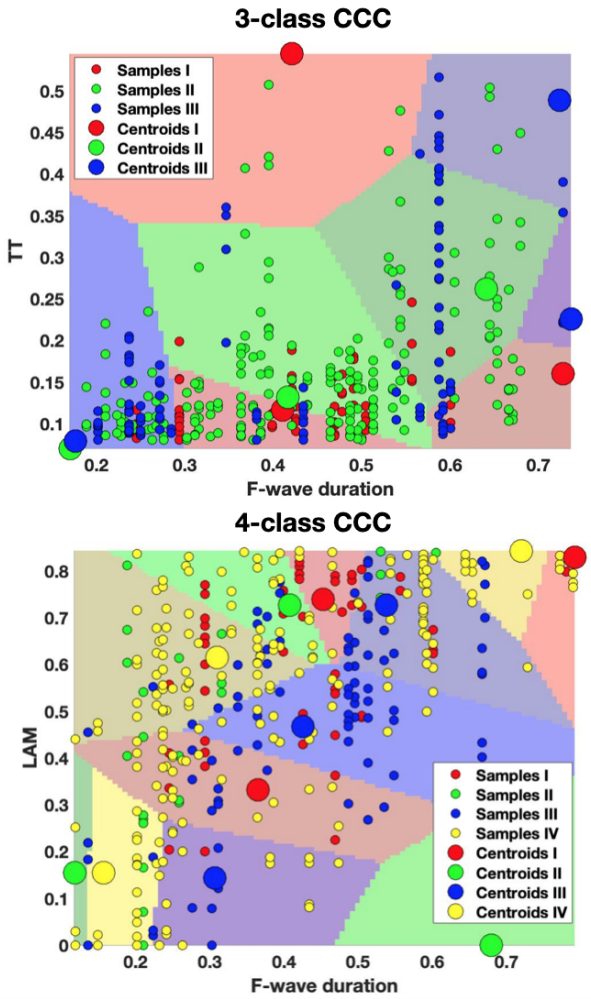

Figure 2. Examples of the partitioning of the feature space into clusters and associated clinical classes together with the position of the test set samples. The color of the big circles (centroids) and small circles (test samples) represent the clinical class. The different shades of a given class's color represent the associated cluster. Any test sample that does not have the same color as the area in which it is located was misclassified. Top and bottom panels represent the 3-class and 4-class CCC with 3 clusters for each clinical class, respectively.

that a supervised classifier can potentially identify clinical classes of different AFl mechanisms using the 12-lead ECG, or more precisely a single F-wave. This non-invasive method can help physicians to plan the most appropriate treatment for the patients without the need of prior invasive mapping.

The results obtained in this work, indicate that it is best to stick to the supervised approaches proposed in [4] and [3]. Nevertheless, further tests on clinical data using supervised machine learning algorithms are necessary to effectively assess the proposed classifications.

Acknowledgments

The authors thank Deborah Nairn for her valuable suggestions. The authors gratefully acknowledge financial support from the European Union's Horizon 2020 research and innovation programme under the Marie Skłodowska-Curie grant agreement No.766082 (MY-ATRIA). All authors confirm that they have no other relationships relevant to the contents of this paper to disclose.

References

[1] Cosio FG, Pastora A, Núñeza A, Magalhaesa AP, Awamleh P. Atrial flutter: an update. Rev Esp Cardiol 2006;59(8):816–831.

[2] Markowitz SM, Thomas G, Liu CF, Cheung J, Ip JE, Lerman BB. Atrial tachycardias and atypical atrial flutters: mechanisms and approaches to ablation. Arrhythm Electrophysiol Rev 2019;8(2):131–137.

[3] Luongo G, Schuler S, Rivolta MW, Dössel O, Sassi R, Loewe A. Automatic ECG-based discrimination of 20 atrial flutter mechanisms: Influence of atrial and torso geometries. In 2020 Computing in Cardiology, volume 47. 2020; 1–4.

[4] Luongo G, Schuler S, Luik A, Almeida TP, Soriano DC, Dössel O, Loewe A. Non-invasive characterization of atrial flutter mechanisms using recurrence quantification analysis on the ECG: A computational study. IEEE Trans Biomed Eng 2021;68(3):914–925.

[5] Jacquemet V. An eikonal approach for the initiation of reentrant cardiac propagation in reaction-diffusion models. IEEE Trans Biomed Eng 2010;57(9):2090–2098.

[6] Trächtler J, Oesterlein T, Loewe A, Poremba E, Luik A, Schmitt C, Dössel O. Virtualizing clinical cases of atrial flutter in a fast marching simulation including conduction velocity and ablation scars. CDBME 2015;1(1):405–408.

[7] Krueger MW, Seemann G, Rhode K, Keller DU, Schilling C, Arujuna A, Gill J, O'Neill MD, Razavi R, Dössel O. Personalization of atrial anatomy and electrophysiology as a basis for clinical modeling of radio-frequency ablation of atrial fibrillation. IEEE Trans Med Imaging 2013;32(1):73–84.

[8] Loewe A, Wilhelms M, Dössel O, Seemann G. Influence of chronic atrial fibrillation induced remodeling in a computational electrophysiological model. Biomedizinische Technik 2014;59(S1):S929–S932.

[9] Rivolta MW, Sassi R. Concurrent clustering and classification for assessing the risk of falling during ageing. In Sixth national congress of bioengineering. 2018; 1–4. URL http://hdl.handle.net/2434/582674.

Address for correspondence:

Giorgio Luongo, Karlsruhe Institute of Technology (KIT)
Fritz-Haber-Weg 1, 76131 Karlsruhe, Germany
publications@ibt.kit.edu